CNRS
Centre National de la Recherche Scientifique

INFN
Istituto Nazionale di Fisica Nucleare

Folded Virgo: a preliminary analysis

VIR-0863A-22

P. Stevens, E. Capocasa, M. Barsuglia

Issue: 1

Date: November 16, 2022

VIRGO * A joint CNRS-INFN Project
Via E. Amaldi, I-56021 S. Stefano a Macerata - Cascina (Pisa)
Secretariat: Telephone (39) 050 752 521 * FAX (39) 050 752 550 * Email W3@virgo.infn.it

Contents

1 Introduction

The most straightforward action that can be done to increase the sensitivity of the detector is to increase the arms length. For instance, 3km extension could be added to each arm in order to double their length and, consequently, double the gravitational wave signal amplitude within the detector. Actually, the geographical location of Virgo makes it impossible but there is an idea already proposed by J.R. Sanders and S.W. Ballmer [1] which might allow the use 6km cavities within 3km arms. The idea is to use the current end mirror to send back the beam to the entrance of the arm on a third mirror placed near the input mirror. This set of three mirrors forms an optical resonator which looks like a folded cavity. This
In this preliminary analysis, performed during the Master thesis stage of P.Stevens, the aim is to study the optical behavior of a folded cavity as well as the dominant noises and overall sensitivity of Virgo equipped with them, which we call Folded Virgo.

2 Methods

2.1 Optical design

In this part, we try to characterize a folded cavity (see figure 1) which is an optical resonator constituted by three mirrors. To obtain the optical parameters of this cavity, we use the ABCD-matrix formalism. The six degrees of freedom of our analysis are the radii of curvature of input mirror (ITM), folding mirror (FM), end mirror (ETM) (R_C^{ITM}, R_C^{FM}, R_C^{ETM}), the folded angle (α) and the length of each part of the cavity ($l^{(1)}$, $l^{(2)}$).

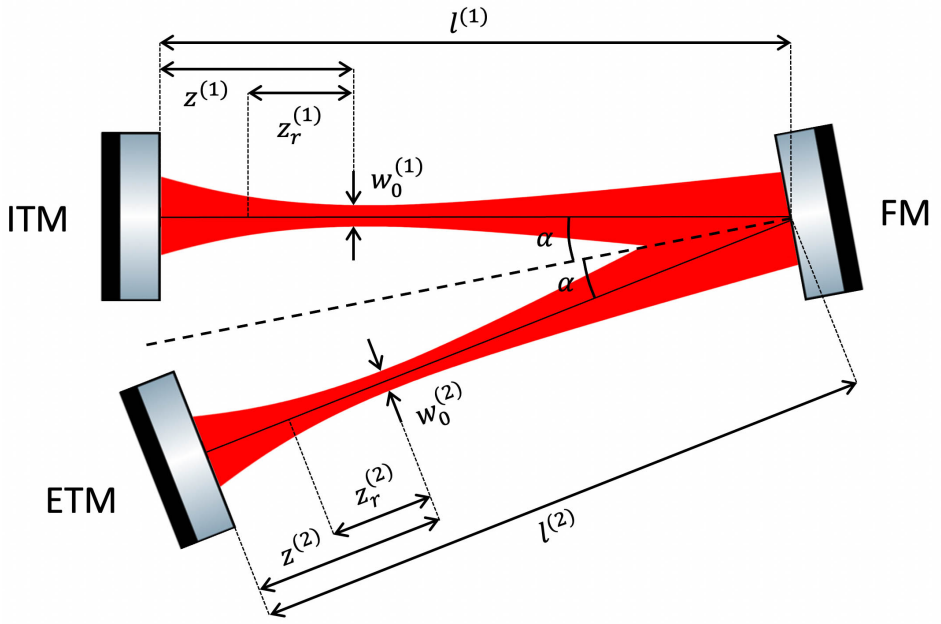

Figure 1: Diagram of the folded cavity with α the folded angle, $w_0^{(1)}$ the beam waist between ITM and FM, $w_0^{(2)}$ the beam waist between FM and ETM, $z^{(1)}$ the distance between $w_0^{(1)}$ position and ITM, $z^{(2)}$ the distance between $w_0^{(2)}$ position and ETM, $z_r^{(1)}$ the beam Rayleigh length between ITM and FM, $z_r^{(2)}$ the beam Rayleigh length between FM and ETM, $l^{(1)}$ the length between ITM and FM and $l^{(2)}$ the length between FM and ETM

The cavity can be considered to be composed of five elements to which a matrix is associated for each : ITM, FM, ETM, space between ITM and FM ($l^{(1)}$), and space between FM and ETM ($l^{(2)}$). The matrices associated

to those elements can be expressed as follows [2] :

$$M_{ITM} = \begin{pmatrix} 1 & 0 \\ -\frac{2}{R_C^{ITM}} & 1 \end{pmatrix}, \quad M_{ETM} = \begin{pmatrix} 1 & 0 \\ -\frac{2}{R_C^{ETM}} & 1 \end{pmatrix}, \quad M_{FM} = \begin{pmatrix} 1 & 0 \\ -\frac{2cos(\alpha)}{R_C^{FM}} & 1 \end{pmatrix} \tag{2.1}$$

$$M_{l^{(1)}} = \begin{pmatrix} 1 & l^{(1)} \\ 0 & 1 \end{pmatrix}, \quad M_{l^{(2)}} = \begin{pmatrix} 1 & l^{(2)} \\ 0 & 1 \end{pmatrix} \tag{2.2}$$

The ABCD-matrix of the folded cavity M_{FC}, can be provided by the product :

$$M_{FC} = \begin{pmatrix} A & B \\ C & D \end{pmatrix} = M_{l^{(1)}} M_{FM} M_{l^{(2)}} M_{ETM} M_{l^{(2)}} M_{FM} M_{l^{(1)}} M_{ITM} \tag{2.3}$$

From M_{FC} coefficients A and D, we can calculate the $g-$factor of the folded cavity by applying the following relation [2] :

$$g = \frac{2 + A + D}{4} \tag{2.4}$$

Then, we can calculate the distance $z^{(1)}$ separating ITM and $w_0^{(1)}$ position, and the Rayleigh length $z_r^{(1)}$.
For this, we use directly the relationships [3] :

$$z^{(1)} = \frac{2B(D-A)}{(D-A)^2 + 4(1-(\frac{A+D}{2})^2)} \tag{2.5}$$

$$z_r^{(1)} = \frac{4|B|\sqrt{1-(\frac{A+D}{2})^2}}{(D-A)^2 + 4(1-(\frac{A+D}{2})^2)} \tag{2.6}$$

Where A, B, C and D are the coefficients of M_{FC} matrix.
Also, it is useful to define the beam parameter at ITM position q_{ITM} for future calculations :

$$q_{ITM} = z^{(1)} + i z_r^{(1)} \tag{2.7}$$

Then, from the Rayleigh length $z_r^{(1)}$, we can derive the waist size :

$$w_0^{(1)} = \sqrt{\frac{\lambda z_r^{(1)}}{\pi}} \tag{2.8}$$

With $\lambda = 1064nm$ the wavelength of the laser used into the interferometer.
Furthermore, the spot radius on ITM and FM can be expressed :

$$w_{ITM} = w_0^{(1)} \sqrt{1 + \left(\frac{z^{(1)}}{z_r^{(1)}}\right)^2} \tag{2.9}$$

$$w_{FM} = w_0^{(1)} \sqrt{1 + \left(\frac{l^{(1)} - z^{(1)}}{z_r^{(1)}}\right)^2} \tag{2.10}$$

With $l^{(1)} - z^{(1)}$ the distance between FM and $w_0^{(1)}$ position.
Finally, to access the spot radius on ETM (w_{ETM}), first, we need to propagate the beam parameter q_{ITM} at ETM position. In order to do this, we need the coefficients A', B', C' and D' of the ABCD-matrix associated to the optical path between ITM and ETM :

$$\begin{pmatrix} A' & B' \\ C' & D' \end{pmatrix} = M_{l^{(2)}} M_{FM} M_{l^{(1)}} M_{ITM} \tag{2.11}$$

Then we apply the following expression :

$$q_{ETM} = \frac{A' q_{ITM} + B'}{C' q_{ITM} + D'} = z^{(2)} + i z_r^{(2)} \tag{2.12}$$

Replacing $z^{(1)}$ and $z_r^{(1)}$ with $z^{(2)}$ and $z_r^{(2)}$ respectively in (2.8) and (2.9) let us find $w_0^{(2)}$ and w_{ETM}.
Note that we could calculate w_{FM} using $w_0^{(2)}$, $z_r^{(2)}$ and $l^{(2)} - z^{(2)}$ thanks to (2.10) to check that the same result is found as before.

In figure 2 we plot an example of beam profile for a given set of cavity parameters.

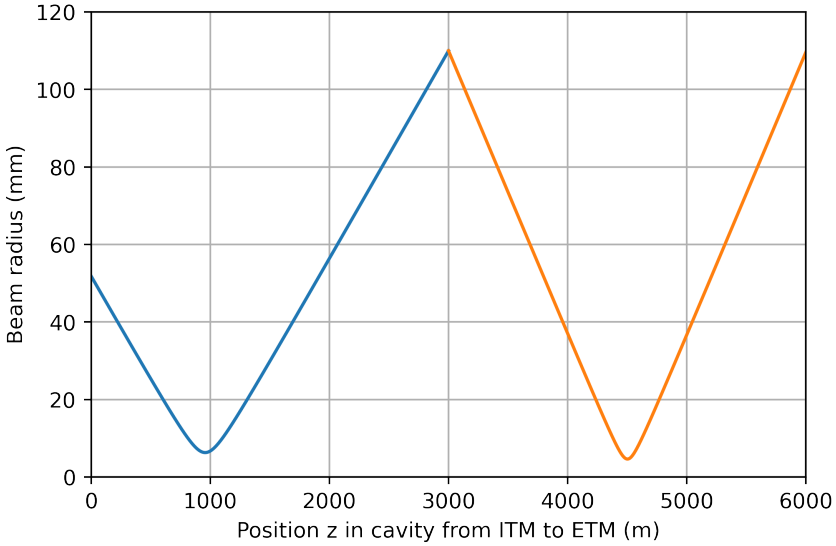

Figure 2: Evolution of beam radius through the folded cavity ($R_C^{ITM} = 971m$, $R_C^{FM} = 1736m$, $R_C^{ETM} = 1500m$, $\alpha = 86\mu rad$ and $l^{(1)} = l^{(2)} = 3000m$). Blue line describes beam portion between ITM (0m) and FM (3000m). Orange line describes beam portion between FM and ETM (6000m).

Another parameter which could be interesting to calculate is the radius of curvature of beam wavefront at FM position (R_{Beam}^{FM}).
Using the definition :

$$\frac{1}{q_{FM}} = \frac{1}{R_{Beam}^{FM}} - i\frac{\lambda}{\pi w_{FM}^2} \tag{2.13}$$

With q_{FM} the beam parameter at FM position which can be computed by propagating q_{ITM} at FM position using the same method which allowed us to find q_{ETM}.
From (2.13), we can extract the radius of curvature :

$$R_{Beam}^{FM} = \frac{1}{Re(\frac{1}{q_{FM}})} \tag{2.14}$$

2.2 Noises

In this part, we are interested in the dominant sources of noise between 10Hz and 10kHz (coating Brownian noise, quantum noise, suspension thermal noise and Newtonian noise) and we derive the formula with which each noise source can be calculated for Folded Virgo.

2.2.1 Coating Brownian noise

The coating Brownian noise S for a single mirror can be expressed [4] :

$$S = \sqrt{\frac{4k_bT}{f}\frac{1-\sigma^2}{\sqrt{\pi}E_0 w}\phi(f)} \tag{2.15}$$

With k_b the Boltzmann constant, T the mirror temperature, f the frequency, σ the Poisson coefficient, E_0 the Young modulus, $\phi(f)$ the loss angle and w the beam spot radius on the mirror.

The total noise of the folded cavity S_{FC} is the contribution of the three mirrors :

$$S_{FC} = \sqrt{S_{ITM}^2 + 6S_{FM}^2 + S_{ETM}^2} \tag{2.16}$$

Where S_{ITM}, S_{FM} and S_{ETM} are the individual coating noise of ITM, FM and ETM, respectively.
Note that the total noise is calculated as the square root of the sum of individual noises squared because each mirror noise is not correlated with the others.
The coefficient 6 arises from the particular role the FM plays within the folded cavity. Intrinsically, the coating Brownian noise of this mirror needs to be multiplied by a factor 3/2 compared to that of ITM or ETM [1]. Also, for one complete beam round trip within the cavity, the FM is "seen" two times and those two contributions are coherent, meaning that a coefficient 2 to the square must be added.
So, the total coefficient by which the FM coating noise must be weighted is : $\frac{3}{2}2^2 = 6$.

Thanks to (2.15) we can rewrite (2.16) :

$$S_{FC} = \sqrt{\frac{4k_bT}{f}\frac{1-\sigma^2}{\sqrt{\pi}E_0}\phi(f)}\sqrt{\frac{1}{w_{ITM}} + \frac{6}{w_{FM}} + \frac{1}{w_{ETM}}} \tag{2.17}$$

At this point, we choose to compare S_{FC} to the coating Brownian noise of Advanced Virgo + (AdV+) Fabry-Perot cavity which expresses :

$$S_{AdV+} = \sqrt{\frac{4k_bT}{f}\frac{1-\sigma^2}{\sqrt{\pi}E_0}\phi(f)}\sqrt{\frac{1}{w_{ITM}^{AdV+}} + \frac{1}{w_{ETM}^{AdV+}}} \tag{2.18}$$

We make the assumption that the folded cavity use the same mirror and coating materials as AdV+ and both of them are at the same temperature. So the two cavities share the same values of σ, E_0, $\phi(f)$ and T. Also, we choose the folded cavity to be twice as long as AdV+, so the gravitational wave signal will have an amplitude twice as large in it than in AdV+. Therefore, it is irrelevant to directly compare the noises associated with those two cavities. Instead, we compare the noise to signal ratio of each cavity by defining :

$$r = \frac{\frac{S_{FC}}{2A}}{\frac{S_{AdV+}}{A}} = \frac{1}{2}\sqrt{\frac{\frac{1}{w_{ITM}} + \frac{6}{w_{FM}} + \frac{1}{w_{ETM}}}{\frac{1}{w_{ITM}^{AdV+}} + \frac{1}{w_{ETM}^{AdV+}}}} \tag{2.19}$$

Where A is the amplitude of a gravitational wave signal.
Leaving temperature dependency in (2.19) let us the possibility to study the impact of FM cooling.
Hence, we define a second ratio :

$$r(T_{FM}) = \frac{1}{2}\sqrt{\frac{\frac{T_C}{w_{ITM}} + \frac{6T_{FM}}{w_{FM}} + \frac{T_C}{w_{ETM}}}{\frac{T_C}{w_{ITM}^{AdV+}} + \frac{T_C}{w_{ETM}^{AdV+}}}} \tag{2.20}$$

With T_{FM} the temperature of FM (which can be modulated to study the impact of cooled FM on overall coating Brownian noise) and T_C the temperature of all other mirrors (which is fixed to room temperature : 290K).

We want to minimize the noise of folded cavity meaning that we want to minimize r and $r(T_{FM})$. In order to do this, we need to maximize w_{ITM}, w_{FM}, w_{ETM} and set T_{FM} as low as possible (T_C, w_{ITM}^{AdV+} and w_{ETM}^{AdV+} being fixed). We saw in optical design part how to calculate w_{ITM}, w_{FM} and w_{ETM}, so we wrote an optimisation Python code to find the parameters of the cavity configuration which have the lowest coating thermal noise : we set an interval of radius of curvature to test for each mirror and the code computes the coating noise associated to each combination then searches which one have the lowest noise.
To comply with technical constraints of the interferometer, we only consider configurations which satisfy the following conditions : $w_{ITM} \leq 52mm$, $w_{FM} \leq 110mm$ and $w_{ETM} \leq 110mm$.

First, we do an initial analysis. The radii of curvature of the three mirrors vary from $1m$ to $10001m$ by $20m$ steps. This leads to 120 millions configurations tested. The folded angle is $\alpha = 86\mu rad$ (corresponds to an arbitrarily fixed spacing distance between ITM and ETM of $50cm$), the cavity length is taken as $l^{(1)} = l^{(2)} = 3000m$ and the selected temperatures are $T_C = 290K$, $T_{FM} = 120K$ then $T_{FM} = 20K$.
The results are shown in column "Initial analysis" of table 1.

A second analysis, more precise, is performed around the radii of curvatures found in the first one. The only change compared to the first analysis is the step length between two tested radii. Here, by $1m$ steps we choose to test radii of curvature which are in an interval of $\pm 100m$ around values found on first analysis. So, R_C^{ITM} varies from $841m$ to $1041m$, R_C^{FM} varies from $1661m$ to $1861m$ and R_C^{ETM} varies from $1381m$ to $1581m$.
The results of this second analysis are shown in column "Second analysis" of table 1. We can see that, during the optimisation, the limit beam radii ($52mm$ on ITM, $110mm$ on FM and ETM) have been reached which is consistent with the behavior of coating noise as function of beam size on mirrors. Furthermore the $g-$factor of the folded cavity is lower than AdV+ Fabry Perot cavities ($g^{AdV+} = 0.95$) indicating greater stability.
If we let the FM is at room temperature, the coating noise of the folded cavity is approximately 20 % lower that AdV+ one but if the FM is cooled to 20K, the coating noise of the folded cavity drops to half AdV+ one which is a significant improvement.

Parameter	Initial analysis	Second analysis
R_C^{ITM}	$941m$	$971m$
R_C^{FM}	$1761m$	$1736m$
R_C^{ETM}	$1481m$	$1500m$
w_{ITM}	$49mm$	$52mm$
w_{FM}	$108mm$	$110mm$
w_{ETM}	$105mm$	$110mm$
$g - factor$	0.92	0.93
r	82.6%	81.4%
$r(T_{FM} = 120K)$	65.1%	63.8%
$r(T_{FM} = 20K)$	52.0%	50.7%

Table 1: Two optimisation analysis results for folded cavity

Also, in figure 3, we plot the evolution of $r(T_{FM})$ for the optimised set of radii of curvature found in second analysis.

Finally, it is interesting to note that, within this resonator, the wavefront radius of curvature is not equal to the mirror radius of curvature at FM position. Using (2.14), we find that $R_{Beam}^{FM} = 2050m \neq R_C^{FM} = 1736m$.

2.2.2 Quantum noise

The radiation pressure noise of a dual recycled Fabry-Perot Michelson interferometer can be written as :

$$S_{rp}^{FP} = \frac{2C}{m} \tag{2.21}$$

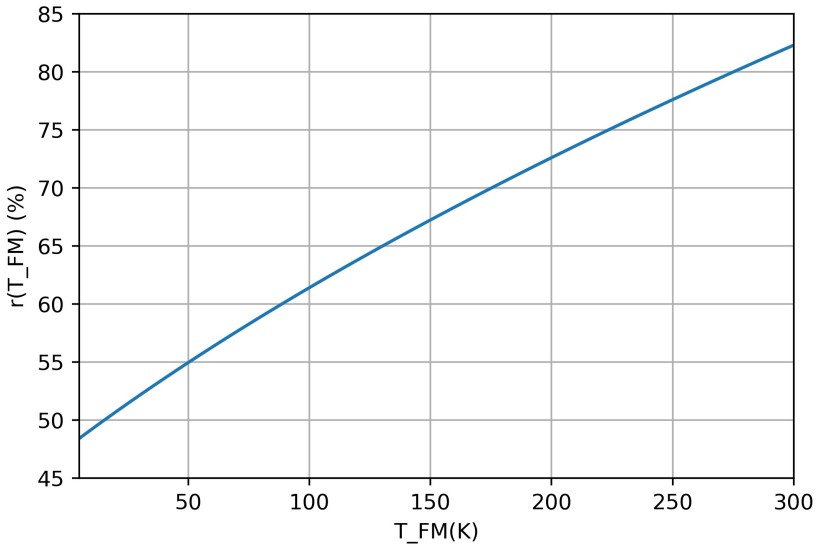

Figure 3: Evolution of $r(T_{FM})$ ($T_C = 290K$, $R_C^{ITM} = 971m$, $R_C^{FM} = 1736m$, $R_C^{ETM} = 1500m$, $\alpha = 86\mu rad$ and $l^{(1)} = l^{(2)} = 3000m$)

Where C is an appropriate value and the factor 2 has been made explicit to point out the equal contribution of the two cavity mirrors.
In the case of Fabry Perot cavities with mirrors of different masses, (2.21) can be rewritten :

$$S_{rp}^{FP} = \frac{C}{m_{ITM}} + \frac{C}{m_{ETM}} \equiv \frac{2C}{m^{FP}} \tag{2.22}$$

From which we can deduce :

$$m^{FP} = \frac{2}{\frac{1}{m_{ITM}} + \frac{1}{m_{ETM}}} \tag{2.23}$$

Following the same procedure, radiation pressure noise in the case of folded cavity can be computed as :

$$S_{rp}^{FC} = \frac{C}{m_{ITM}} + \frac{2C}{m_{FM}} + \frac{C}{m_{ETM}} \equiv \frac{2C}{m^{FC}} \tag{2.24}$$

Where the coefficient 2 for FM term arises from the two contributions of FM during one beam round trip.
Finally, from (2.24) we can deduce :

$$m^{FC} = \frac{2}{\frac{1}{m_{ITM}} + \frac{2}{m_{FM}} + \frac{1}{m_{ETM}}} \tag{2.25}$$

2.2.3 Suspension thermal noise

The suspension thermal noise of a folded cavity is constituted by the incoherent contribution of ITM, FM and ETM suspensions. Note however that the FM contributes two times coherently.
The total suspension thermal noise is the incoherent sum of each arm, so the total strain noise expresses :

$$S_{susp} = \frac{\sqrt{2\left((S_{susp}^{ITM})^2 + (2S_{susp}^{FM})^2 + (S_{susp}^{ETM})^2\right)}}{L_{FC}} \tag{2.26}$$

Where L_{FC} is the length of the folded cavity and S_{susp}^{ITM}, S_{susp}^{FM} and S_{susp}^{ETM} are the individual suspension thermal noises of ITM, FM and ETM, respectively.

2.2.4 Newtonian noise

For the Newtonian noise in a folded cavity, we make the assumption that ITM and ETM are close enough so that their environment may be considered to be the same. Therefore, the contribution of those two mirrors add up coherently. As for the suspension thermal noise, the FM contributes two times coherently. However, the contribution of ITM / ETM is not correlated to FM one.
The total Newtonian strain noise of the interferometer being the incoherent sum of each arm, it expresses :

$$S_{nn} = \frac{\sqrt{2\left((S_{nn}^{ITM} + S_{nn}^{ETM})^2 + (2S_{nn}^{FM})^2\right)}}{L_{FV}} \tag{2.27}$$

With S_{nn}^{ITM}, S_{nn}^{FM} and S_{nn}^{ETM} the individual Newtonian noises of ITM, FM and ETM, respectively.
Following the same reasoning, we can express the AdV+ Newtonian noise :

$$S_{nn}^{AdV+} = \frac{\sqrt{2\left(\left(S_{nn}^{ITMAdV+}\right)^2 + \left(S_{nn}^{ETMAdV+}\right)^2\right)}}{L_{FP}^{AdV+}} \tag{2.28}$$

With $S_{nn}^{ITMAdV+}$ and $S_{nn}^{ETMAdV+}$ the individual Newtonian noises of AdV+ ITM and ETM, respectively, and L_{FP}^{AdV+} the length of AdV+ cavities.
Then, we can define the ratio :

$$r_{nn} = \frac{S_{nn}}{S_{nn}^{AdV+}} \tag{2.29}$$

Assuming that each individual mirror have the same Newtonian noise $S_{nn}^{ITMAdV+} = S_{nn}^{ETMAdV+} = S_{nn}^{ITM} = S_{nn}^{FM} = S_{nn}^{ETM} = S_{nn}^{mir}$ and knowing that $L_{FV} = 6000m$ and $L_{FP}^{AdV+} = 3000m$, (2.29) becomes :

$$r_{nn} = \frac{3000}{6000}\sqrt{\frac{2\left((S_{nn}^{mir} + S_{nn}^{mir})^2 + (2S_{nn}^{mir})^2\right)}{2\left(\left(S_{nn}^{mir}\right)^2 + \left(S_{nn}^{mir}\right)^2\right)}} = 1 \tag{2.30}$$

So, finally, we expect the same Newtonian noise for AdV+ and Folded Virgo.

3 Simulation results

3.1 Noises

To perform the noise simulations, we used GWINC which has been modified to take into account the new noises formula derived in section 2.2.
Also, we used results of our second optimisation analysis (see table 1) to parametrize the folded cavities.
On each strain noise simulation, we have also plotted AdV+ O5 case so that we can compare the behavior of Folded Virgo to the best update currently planned.
Note that for all the simulations, we arbitrarily fixed the recycling mirrors transmission coefficient to 0.2.

3.1.1 Coating Brownian noise

On figure 4, we can see that the simulations correspond well with the analytical predictions expressed in table 1. Actually, if we calculate the ratio between blue curve and red curve for a given frequency, we find the same value as r (see second analysis of table 1). And if we calculate the ratio between green curve and red curve for a given frequency, we find the same value as $r(T_{FM})$ (see second analysis of table 1).
Still on figure 4, we can see that Folded Virgo noise curves go up at high frequency. This is because the frequency spectral range of AdV+ is twice as large as Folded Virgo (as Folded Virgo uses cavities twice as long as AdV+). Therefore, the first resonance peak of Folded Virgo is at lower frequency than AdV+ which explains that we see this slight rise around 10kHz for Folded Virgo cases.

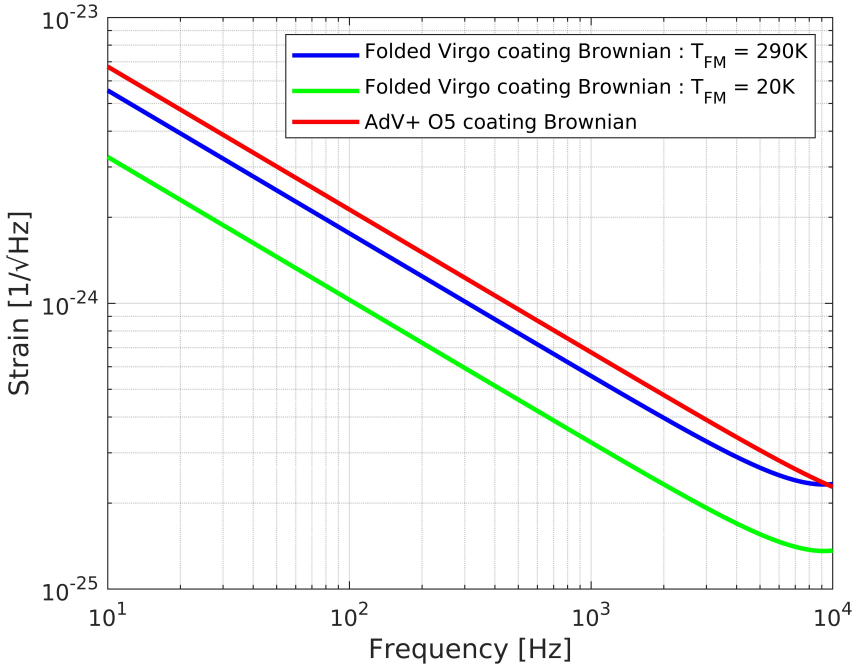

Figure 4: Coating Brownian strain noise for Folded Virgo and AdV+ O5 run. For Folded Virgo, two results are presented : the blue line corresponds to a FM at room temperature (290K), the green line corresponds to cooled FM (20K).

3.1.2 Quantum noise

The simulation results of quantum noise (figure 5) show a significant improvement at low frequency. Because of the addition of a third mirror, the radiation pressure noise (inversely proportional to the sum of mirrors masses as we can see in (2.21)) decreases. For Folded Virgo simulations, we kept ITM and ETM masses of AdV+ O5 ($m_{ITM}^{AdV+} = m_{ITM} = 40kg$, $m_{ETM}^{AdV+} = m_{ETM} = 100kg$) and choose to set $m_{FM} = m_{ETM} = 100kg$.

3.1.3 Suspension thermal noise

For suspension thermal noise (figure 6), we can see that the noise of Folded Virgo is reduced compared to AdV+ but keeps the same resonance peak frequencies which is consistent since we assumed that the same mirror suspensions are used for Folded Virgo and AdV+.

3.1.4 Newtonian Noise

The Newtonian noise (figure 7) of Folded Virgo and AdV+ are the same which is consistent with (2.30).

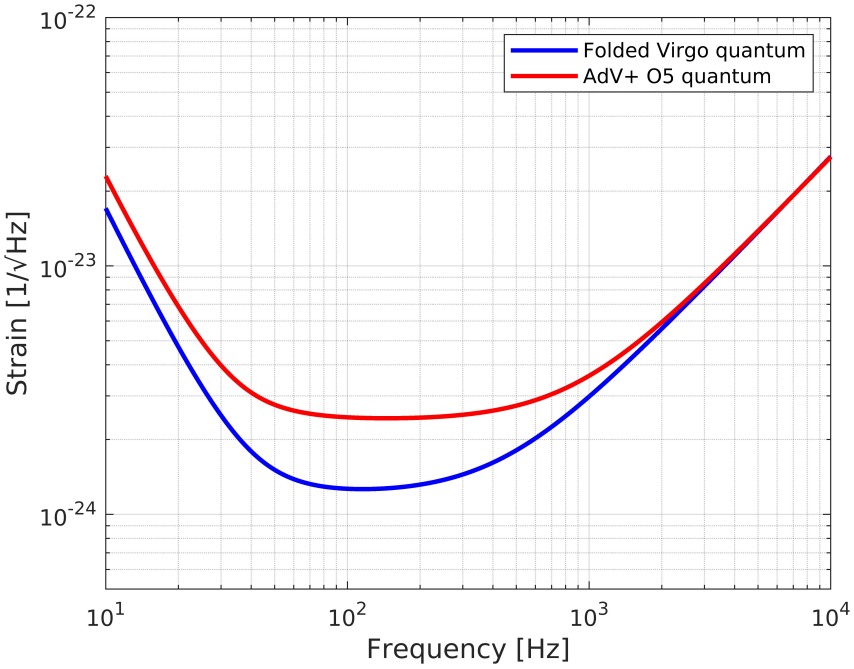

Figure 5: Quantum strain noise of AdV+ O5 run and Folded Virgo.

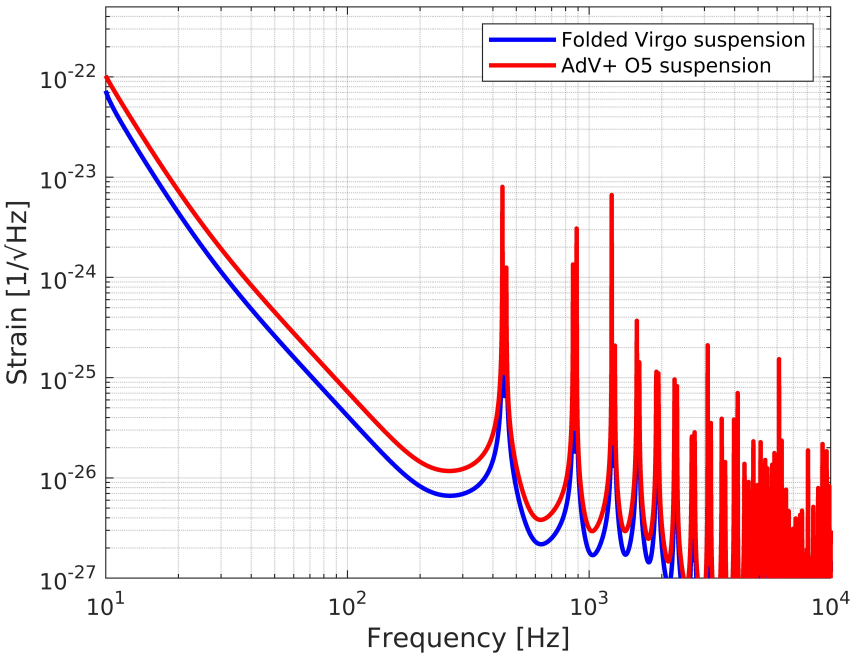

Figure 6: Suspension thermal strain noise of AdV+ O5 run and Folded Virgo.

3.2 Folded Virgo sensitivity

The decrease of most noises previously presented leads to a significant improvement of overall sensitivity for Folded Virgo compared to AdV+ O5. On figure 8 is presented the noise budget of Folded Virgo. For this simulation, we choose to let the FM at room temperature so the thermal Brownian noise corresponds to blue line case of figure 4.

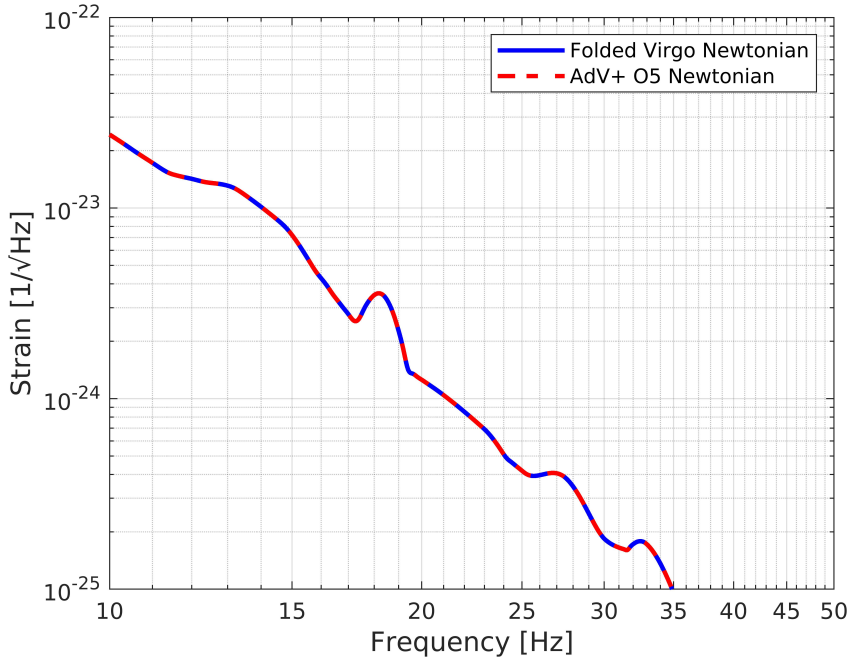

Figure 7: Newtonian strain noise of AdV+ O5 run and Folded Virgo.

More quantitatively, we can compare Folded Virgo to AdV+ thanks to the BNS and BBH ranges presented in table 2. 45% improvement is made for BNS range and 31% is made for BBH range. This can lead to a number of detected BNS events three times larger for Folded Virgo than for AdV+ O5 and 2.2 times larger for BBH events.

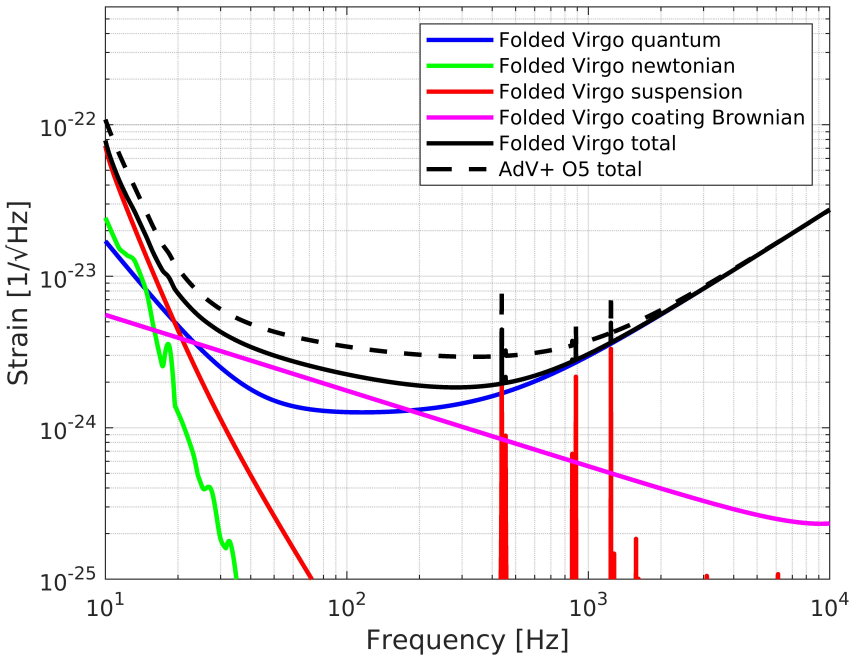

Figure 8: Noise Budget and overall sensitivity of Folded Virgo compared to AdV+ O5 run sensitivity.

Interferometer	BNS range	BBH range
Folded Virgo ($T_{FM} = 290K$)	343.69 Mpc	2.61 Gpc
AdV+ O5	236.65 Mpc	1.98 Gpc

Table 2: Simulations results of Folded Virgo compared to AdV+ O5 run

3.3 Cavity misalignment

We can study the sensitivity of the folded cavity to mirror misalignment thanks to the simulation software Finesse. The aim of those simulations is to measure the laser power inside the cavity as function of mirror misalignment angle (mirrors are rotated one by one around a single axis). To compare to a reference, we made a simulation for each mirror of the folded cavity and AdV+ Fabry Perot cavity.
For those simulations, we choose the following parameters :

- Parameters used for AdV+ Fabry Perot cavity simulations :
  - Input laser power : $P = 1W$
  - Input mirror : $R_C^{ITM} = 1067m$, $R^{ITM} = 0.986$, $T^{ITM} = 0.014$
  - End mirror : $R_C^{ETM} = 1969m$, $R^{ETM} = 0.999$, $T^{ETM} = 0.001$
  - Cavity length : $l = 3000m$
- Parameters used for folded cavity simulations :
  - Input laser power : $P = 1W$
  - Input mirror : $R_C^{ITM} = 971m$, $R^{ITM} = 0.986$, $T^{ITM} = 0.014$
  - Folding mirror : $R_C^{FM} = 1736m$, $R^{FM} = 1$, $T^{FM} = 0$
  - End mirror : $R_C^{ETM} = 1500m$, $R^{ETM} = 0.999$, $T^{ETM} = 0.001$
  - Folding angle : $\alpha = 86\mu rad$
  - Cavity length between ITM and FM : $l^{(1)} = 3000m$
  - Cavity length between FM and ETM : $l^{(2)} = 3000m$

R and T correspond to reflection and transmission coefficients (respectively) of mirrors.

On figure 9 are presented the results of the Finesse simulations. We can see that, for both cavities, ITM and ETM behave in the same way. Note that the folded cavity is slightly more sensitive to ETM misalignment but not significantly. For FM tilt, we can see that the stability interval is approximately twice as small as for ETM which should not be problematic to maintain the cavity in a resonant state.

4 Further upgrade

In part 2.2.1, we performed an optimisation to find which cavity parameters provide maximum beam spots on mirrors and, consequently, the minimum coating Brownian noise. For this optimisation we limited the beam spot radius on ITM to $52mm$ but we see on Folded Virgo noise budget (figure 8) that the overall sensitivity is still limited by coating Brownian noise around 50Hz / 100Hz.
So we can consider changing the ITM to have the same technical constraints as on ETM and FM in order to expand the spot radius up to $110mm$ (which would lead to an additional decrease of coating Brownian noise). Finally, to have the minimal noise, we could combine this increase of spot size on ITM and the cooling of the FM. On table 3 are presented the results of an optimisation for which the spot radius on ITM is limited to $110mm$.
The noise simulations indicate that, for FM at room temperature, the noise slightly decreases by expanding the

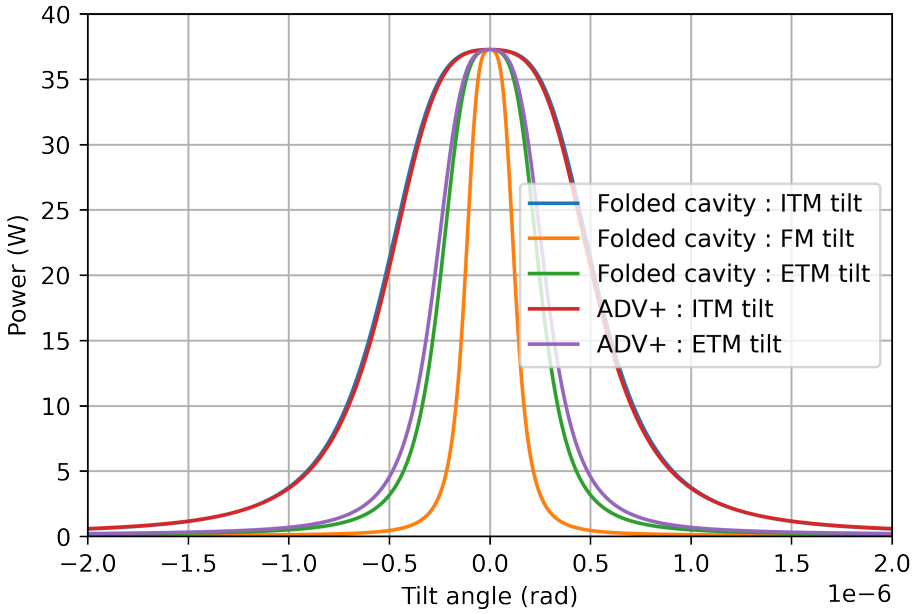

Figure 9: Simulated power curves within folded cavity and AdV+ Fabry Perot cavity as function of individual mirror tilt angle

spot on ITM (see table 4 and blue / purple lines of figure 10). But the most interesting result is the strain noise corresponding to an expanded spot size on ITM combined to a cooled FM (see pink line of figure 10), this noise is significantly lower than all others and could increase overall detector sensitivity over a wide low frequency band.

Parameter	Folded Virgo ($w_{ITM}^{lim} = 110mm$)
R_C^{ITM}	$1502.7m$
R_C^{FM}	$1502.7m$
R_C^{ETM}	$1502.7m$
w_{ITM}	$110mm$
w_{FM}	$110mm$
w_{ETM}	$110mm$
$g - factor$	0.97
r	76.3%
$r(T_{FM} = 120K)$	57.2%
$r(T_{FM} = 20K)$	47.9%

Table 3: Cavity parameters for Folded Virgo with a limit beam spot size on ITM set to $110mm$

5 Conclusion

To conclude, the folded cavity does not behave as simply as a Fabry Perot cavity, especially because of its folding mirror which behaves physically differently from ITM and ETM. However, this folded cavity is no more unstable that Fabry Perot cavity which will be used by AdV+.
Then, the use of folded cavities within the detector reduces most dominant noise sources leading to an improved overall sensitivity which could allow to detect 3 times more BNS events and 2.2 times more BBH events that

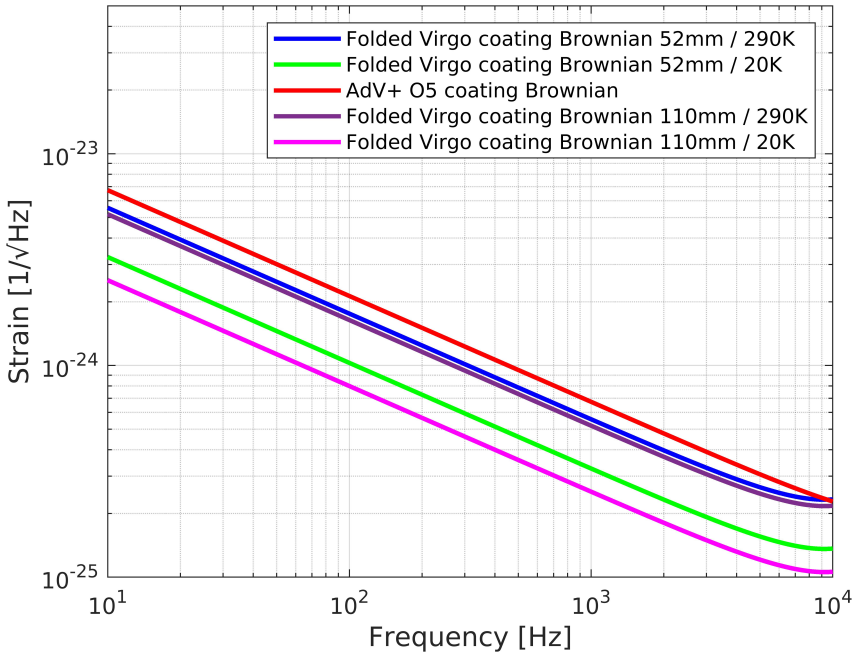

Figure 10: Coating Brownian strain noise for different configurations of Folded Virgo upgrade (52mm / 110mm beam radius on ITM, and FM at 20K / 290K) compared to AdV+ O5 run

Interferometer	BNS range	BBH range
Folded Virgo ($w_{ITM} = 110mm$, $T_{FM} = 290K$)	357.22 Mpc	2.68 Gpc
Folded Virgo ($w_{ITM} = 52mm$, $T_{FM} = 290K$)	343.69 Mpc	2.61 Gpc
AdV+ O5	236.65 Mpc	1.98 Gpc

Table 4: Simulation ranges results for large ITM beam spot upgrade compared to previous configurations

AdV+ (considering the simplest upgrade configuration : small spot size in ITM, and FM at room temperature). Finally, this upgrade leaves the door open for other improvements like a cryogenized FM or a widened beam on ITM.

6 Acknowledgements

P.S internship recived financial support by LabEx UnivEarthS (ANR-10-LABX-0023 and ANR-18-IDEX-0001)

References

[1] J.R. Sanders and S.W. Ballmer, Folding gravitational-wave interferometers, 2016 2, 5

[2] C. Bond, D. Brown, A. Freise, K.A. Strain, Interferometer techniques for gravitational-wave detection, 2016 3

[3] D. Fiorucci, Feasibility study of an optical resonator for applications in neutral-beam injection systems for the next generation of nuclear fusion reactors, 2015 3

[4] M. Blom, Seismic attenuation for Advanced Virgo Vibration isolation for the external injection bench, 2015 5